

# New structural model for GeO<sub>2</sub>/Ge interface: A first-principles study

Shoichiro Saito\* and Tomoya Ono

*Graduate School of Engineering, Osaka University*

(Dated: March 3, 2018)

## Abstract

First-principles modeling of a GeO<sub>2</sub>/Ge(001) interface reveals that sixfold GeO<sub>2</sub>, which is derived from cristobalite and is different from rutile, dramatically reduces the lattice mismatch at the interface and is much more stable than the conventional fourfold interface. Since the grain boundary between fourfold and sixfold GeO<sub>2</sub> is unstable, sixfold GeO<sub>2</sub> forms a large grain at the interface. On the contrary, a comparative study with SiO<sub>2</sub> demonstrates that SiO<sub>2</sub> maintains a fourfold structure. The sixfold GeO<sub>2</sub>/Ge interface is shown to be a consequence of the ground-state phase of GeO<sub>2</sub>. In addition, the electronic structure calculation reveals that sixfold GeO<sub>2</sub> at the interface shifts the valence band maximum far from the interface toward the conduction band.

PACS numbers: 68.35.-p, 77.55.dj, 61.50.Ks

---

\* saito@cp.prec.eng.osaka-u.ac.jp

1 With the continued scaling of Si metal-oxide-semiconductor (MOS) devices, it is becoming  
2 increasingly difficult to enhance device performance; therefore, new channel materials have  
3 been explored. Ge is considered as one of the best channel materials for obtaining high  
4 performance MOS devices due to its higher carrier mobility. The narrower band gap of  
5 Ge is also attractive since lower operation voltage lowers energy consumption. To fabricate  
6 high performance devices with a Ge channel, one of the most crucial challenges is fabricating  
7 an insulator with superior interface properties since the termination of the surface states is  
8 important for device reliability. So far, various insulators have been examined, for example,  
9 GeO<sub>2</sub> [1, 2], Ge<sub>3</sub>N<sub>4</sub> [3], and high-*k* oxides [4–6]. Among these insulators, GeO<sub>2</sub> is the most  
10 fundamental and important, similar to SiO<sub>2</sub> in Si MOS technology, because it exists even  
11 in high-*k* oxide/Ge interfaces. A considerable number of studies have been conducted on  
12 the process of developing high quality GeO<sub>2</sub>/Ge interfaces, and several groups have reported  
13 that GeO<sub>2</sub>/Ge interfaces, fabricated by conventional dry oxidation, have a low interface trap  
14 density (mid 10<sup>10</sup>–10<sup>11</sup> cm<sup>-2</sup>eV<sup>-1</sup>) [1, 2]. Houssa *et al.* simulated the density of Ge dangling  
15 bonds at the GeO<sub>2</sub>/Ge interface as a function of the oxidation temperature, by combining  
16 viscoelastic data of GeO<sub>2</sub> and the modified Maxwell’s model, and claimed that the density  
17 of Ge dangling bonds is less than that of Si dangling bonds at the SiO<sub>2</sub>/Si interface [7].  
18 Their results are in good agreement with other reported results [1, 2].

19 Interface stress between a semiconductor and an oxide is considered as one of the origins  
20 of interface defects. Kageshima and Shiraishi predicted that Si atoms are emitted from the  
21 interface to release stress induced by the lattice-constant mismatch between SiO<sub>2</sub> and Si,  
22 although the dangling bonds remain after Si atom emission [8]. On the other hand, we cal-  
23 culated the probability of Ge atom emission from a GeO<sub>2</sub>/Ge interface by using the interface  
24 model proposed by Kageshima and Shiraishi and found that hardly any Ge atoms are emit-  
25 ted from the GeO<sub>2</sub>/Ge interface [9]. We concluded that the flexibility of the O-Ge-O bonds  
26 contributes to the relaxation of interface stress, resulting in a GeO<sub>2</sub>/Ge interface that is su-  
27 perior to the SiO<sub>2</sub>/Si one. Watanabe *et al.* claimed, using the classical molecular-dynamics  
28 simulation, that the narrow equilibrium Ge-O-Ge bond angles contribute to the reduction in  
29 compressive stress in GeO<sub>2</sub> films as well as flexible O-Ge-O bonds [10]. Although a consider-  
30 able number of first-principles studies on the GeO<sub>2</sub>/Ge interface have been conducted based  
31 on the calculations on SiO<sub>2</sub>/Si interfaces [7, 11–15], the atomic and electronic structures  
32 of the GeO<sub>2</sub>/Ge interface have not been identified experimentally because GeO<sub>2</sub> is both

33 water-soluble and thermally unstable at elevated temperatures.

34 We propose a complete ordered  $\text{GeO}_2/\text{Ge}(001)$  interface structure with minimum lattice  
35 mismatch. Our interface model consists of sixfold  $\text{GeO}_2$ , which is derived from cristobalite  
36 and is different from rutile, on a  $\text{Ge}(001)$  substrate. The sixfold  $\text{GeO}_2/\text{Ge}$  interface is more  
37 stable by 1.92 eV than the conventional fourfold  $\text{GeO}_2/\text{Ge}$  interface. The lattice mismatch  
38 between sixfold  $\text{GeO}_2$  and Ge ( $\sim 5\%$ ) is much smaller than that between fourfold  $\text{GeO}_2$   
39 and Ge ( $\sim 17\%$ ). By examining a mixed fourfold and sixfold  $\text{GeO}_2/\text{Ge}$  interface model, we  
40 find that sixfold  $\text{GeO}_2$  exists as a large grain at the  $\text{GeO}_2/\text{Ge}$  interface. On the contrary,  
41  $\text{SiO}_2$  at the  $\text{SiO}_2/\text{Si}$  interface maintains a fourfold structure. A comparative study of the  
42 electronic structures of the sixfold and fourfold  $\text{GeO}_2/\text{Ge}$  interfaces shows that the valence  
43 band maximum (VBM) far from the interface varies due to the existence of sixfold  $\text{GeO}_2$  at  
44 the interface.

45 Our first-principles calculation method is based on the real-space finite-difference ap-  
46 proach [16–18], which enables us to determine a self-consistent electronic ground state  
47 with a high degree of accuracy using a timesaving double-grid technique [17, 18]. The  
48 norm-conserving pseudopotentials [19] of Troullier and Martins [20] are used to describe the  
49 electron-ion interaction and are transformed into the computationally efficient Kleinman-  
50 Bylander separable form [21], using the  $s$  and  $p$  components as nonlocal components for H,  
51 O, and Si, and the  $s$ ,  $p$ , and  $d$  components as nonlocal components for Ge. Exchange and  
52 correlation effects are treated using the local density approximation [22]. The coarse grid  
53 spacing of  $\sim 0.13$  Å, which corresponds to the plane wave cutoff energy of  $\sim 112$  Ry, is used  
54 for all of our calculations. We first examine the atomic structures of  $\text{GeO}_2$  and  $\text{SiO}_2$  bulks in  
55 the cristobalite phases ( $c\text{-GeO}_2$  and  $c\text{-SiO}_2$ ) under pressure along the  $a$ -axis because these  
56 structures correspond to the directions parallel to the interface when the oxides are piled  
57 on the (001) surface. The  $c\text{-GeO}_2$  ( $c\text{-SiO}_2$ ) structure is tetragonal with four  $\text{GeO}_2$  ( $\text{SiO}_2$ )  
58 molecules per unit cell, and  $4 \times 4 \times 3$   $k$ -point grids in the Brillouin zone are taken into  
59 account. The  $c\text{-GeO}_2$  structure at the equilibrium point is shown in Fig. 1(a). The equi-  
60 librium lattice parameters of  $c\text{-GeO}_2$  and  $c\text{-SiO}_2$ , which are obtained from first-principles  
61 calculation, are listed in Table I. We then compress  $c\text{-GeO}_2$  ( $c\text{-SiO}_2$ ) along the  $a$ -axis by  
62 5-25 (5-35)% from the equilibrium lattice constants and optimize the length of the  $c$ -axis in  
63 increments of 1% to determine the energy minima. We relax all the atoms until all the force  
64 components drop below 0.05 eV/Å.

65 Figures 2(a) and 2(b) show the total energies of  $c$ -GeO<sub>2</sub> and  $c$ -SiO<sub>2</sub> per molecular unit  
 66 as a function of volume. The energy minima of other phases [quartz ( $\square$ ), cristobalite ( $\circ$ ),  
 67 and rutile ( $\triangle$ )] without any constraints are also depicted for comparison. The zero on the  
 68 energy scale is the rutile structure of GeO<sub>2</sub> and the quartz structure of SiO<sub>2</sub>. In this figure,  
 69 the  $c$ -GeO<sub>2</sub> at about  $0.78a_0^{\text{GeO}_2}$  shows a local minimum, where  $a_0^{\text{GeO}_2}$  represents the length of  
 70 the  $a$ -axis of  $c$ -GeO<sub>2</sub> at the equilibrium point (4.818 Å). The atomic structure of the strained  
 71  $c$ -GeO<sub>2</sub> at the local minimum is shown in Fig. 1(b). The  $c$ -GeO<sub>2</sub> under a certain pressure  
 72 transforms into a sixfold structure, which is distinct from the rutile phase, by rotating oxygen  
 73 atoms around the Ge atoms. The energy minimum of sixfold GeO<sub>2</sub> is lower than that of  
 74 fourfold GeO<sub>2</sub> since the zero-temperature phase of GeO<sub>2</sub> has a sixfold rutile structure. The  
 75 critical point between the fourfold and sixfold structures is about  $0.85a_0^{\text{GeO}_2}$ . The arrow on  
 76 the upper horizontal axis corresponds to the lateral length of the Ge(001)-(1 × 1) surface. It  
 77 should be noted that GeO<sub>2</sub> forms a sixfold structure when the length of the  $a$ -axis is equal  
 78 to that of the (1 × 1) surface, while the  $c$ -SiO<sub>2</sub> still maintains a fourfold structure.

79 We next compare the energetic stability of the sixfold GeO<sub>2</sub>/Ge(001) interface with the  
 80 fourfold one since the lattice mismatch between the sixfold GeO<sub>2</sub> and Ge(001) surfaces is  
 81 small ( $\sim 5\%$ ). Figures 3(a) and 3(b) show the fourfold and sixfold GeO<sub>2</sub>/Ge interfaces,  
 82 respectively. The fourfold oxide transforms into a sixfold one by rotating the four oxygen  
 83 atoms around one Ge atom in a Ge(001)-(1 × 1) surface unit. The total energy difference  
 84 between the fourfold and sixfold SiO<sub>2</sub>/Si interfaces are also calculated for comparison. The  
 85 Ge(001)-( $\sqrt{2} \times \sqrt{2}$ ) surface is used for the lateral size of the supercell of the GeO<sub>2</sub>/Ge  
 86 interface, and the length of the supercell perpendicular to the surface is  $5.5a_0^{\text{Ge}}$ , where  $a_0^{\text{Ge}}$  is  
 87 the optimized lattice constant of the Ge bulk (5.578 Å). The model of the interface includes  
 88 seven Ge atomic and two GeO<sub>2</sub> molecular layers, and both sides of the surface are simply  
 89 terminated with H atoms. Eight  $k$ -points in the 1 × 1 lateral unit cell are used for the  
 90 Brillouin zone sampling. All the atoms, except the Ge atoms in the bottom-most layer  
 91 and the H atoms terminating their dangling bonds, are relaxed. The other computational  
 92 details are the same as those used in the bulk calculation. We found that the sixfold GeO<sub>2</sub>/Ge  
 93 interface is more stable by 1.92 eV than the fourfold one because the interface stress between  
 94 GeO<sub>2</sub> and Ge is released by the phase transition into the dense sixfold structure. On the  
 95 other hand, the fourfold  $c$ -SiO<sub>2</sub>/Si interface model is preferable by 1.02 eV compared with  
 96 the sixfold one. Kageshima and Shiraishi reported that Si atoms at the  $c$ -SiO<sub>2</sub>/Si interface

97 are emitted to release interface stress, resulting in a quartz-SiO<sub>2</sub>/Si interface [8]. On the  
98 other hand, hardly any Ge atoms at the *c*-GeO<sub>2</sub>/Ge interface are emitted [9]. Our results  
99 indicate that the sixfold structure contributes to the release of interface stress due to the  
100 lattice mismatch between the *c*-GeO<sub>2</sub> and Ge(001) surfaces.

101 Since the lateral length of the Ge(001)-(1 × 1) surface is longer than that of the sixfold  
102 GeO<sub>2</sub> surface but shorter than that of the fourfold *c*-GeO<sub>2</sub> surface in Fig. 2(a), there is a  
103 possibility that *c*-GeO<sub>2</sub> on the Ge(001) surface is composed of a mixed fourfold and sixfold  
104 structure. We examine the total energies of the supercell doubling of the Ge(001)-( $\sqrt{2} \times \sqrt{2}$ )  
105 surface unit in the two directions, i.e., the supercell contains eight Ge(001)-(1 × 1) units. We  
106 respectively replace one and five neighboring (1 × 1) Ge surface units so that 12.5% and 62.5%  
107 of the Ge(001)-(1 × 1) units are composed of the sixfold structures [Figs. 4(a) and 4(b)]. The  
108 computational procedures are the same as mentioned above. The calculated total energy  
109 differences are summarized in Table II with respect to the ratio of the sixfold coordination.  
110 The fully sixfold GeO<sub>2</sub>/Ge interface is the most stable, and the mixed interface with the  
111 12.5% sixfold structure is even more unstable than the fully fourfold GeO<sub>2</sub>/Ge interface.  
112 The instabilities of the mixed interfaces are attributed to the grain boundaries; the *c*-axis of  
113 the fourfold oxidized region is more than 5% longer than that of the sixfold one. This result  
114 implies that the sixfold oxidized region exists as a large grain at the GeO<sub>2</sub>/Ge interface.

115 Finally, we investigate the effect of the sixfold structure on the variations of the conduction  
116 band minimum (CBM) and VBM along the normal direction to the interface. To suppress  
117 the effect of quantum confinement due to the limitation of substrate thickness, a 12-atomic  
118 layer of the Ge(001) substrate is used. The four GeO<sub>2</sub> molecular layers are piled on the  
119 Ge(001) substrate, and other computational details are the same. It is believed that GeO<sub>2</sub>  
120 is composed of an amorphous structure. Tamura *et al.* found that the band gap of crystalline  
121 GeO<sub>2</sub> is compatible with that of amorphous GeO<sub>2</sub> by using the first-principles calculation  
122 [23]. Therefore, we calculate the electronic structure with and without a sixfold GeO<sub>2</sub>  
123 layer inserted between the crystalline fourfold GeO<sub>2</sub> layer and Ge(001) substrate. The  
124 grain boundary between the sixfold and fourfold structures parallel to the Ge(001) substrate  
125 is stable, although fivefold Ge atoms exist between the sixfold and fourfold boundaries.  
126 Figures 5(a) and 5(b) show the evolution of the CBM and VBM along a direction orthogonal  
127 to the interface plane, respectively. CBM and VBM variations are subtracted from the local  
128 density of states, calculated by integrating them on the plane parallel to the interface based

129 on  $\rho(z, E) = \int |\psi(\mathbf{r}, E)|^2 d\mathbf{r}_{\parallel}$ , with a contour of  $7.94 \times 10^{-5} e/eV/\text{\AA}^3$ . With the fourfold  
130 GeO<sub>2</sub>/Ge interface, the VBM is almost complete at about 5 Å deep from the interface,  
131 which is similar than that with the SiO<sub>2</sub>/Si interface [24], while the CBM saturates within  
132 2 Å. Since the band gap of sixfold GeO<sub>2</sub> is narrower than that of fourfold GeO<sub>2</sub> [25], the  
133 valence electrons in the Ge substrate penetrate sixfold GeO<sub>2</sub> and the interface dipole emerges.  
134 Therefore, the existence of the sixfold GeO<sub>2</sub> layer shifts the VBM far from the interface  
135 toward the conduction band.

136 In summary, we proposed a sixfold GeO<sub>2</sub>/Ge interface, in which the lattice mismatch at  
137 the interface is very small ( $\sim 5\%$ ) and which is energetically much more stable than fourfold  
138 GeO<sub>2</sub>/Ge interfaces. It should be noted that the sixfold structure was found to be a large  
139 grain at the GeO<sub>2</sub>/Ge interface after computing the stability of the mixed fourfold and sixfold  
140 GeO<sub>2</sub>/Ge interface. On the other hand, with SiO<sub>2</sub>, a conventional fourfold structure on the  
141 Si(001) substrate is preferable due to the difficulty in rearranging the rigid O-Si-O bonds  
142 even in the bulk phase. The electronic structure calculation with and without the sixfold  
143 GeO<sub>2</sub> monolayer at the GeO<sub>2</sub>/Ge interface reveals that the VBM far from the interface in  
144 the ultrathin GeO<sub>2</sub> layer ( $\sim 10$  Å) depends on the coordination number of GeO<sub>2</sub>. Our results  
145 provide new insight into a strong candidate of the atomic and electronic structures of the  
146 GeO<sub>2</sub>/Ge interface. We await experimental verification of our prediction.

147 The authors would like to thank Professor Kenji Shiraishi of University of Tsukuba, and  
148 Professor Heiji Watanabe, Professor Yoshitada Morikawa, Professor Takayoshi Shimura, and  
149 Professor Takuji Hosoi of Osaka University for reading the manuscript and for contributing  
150 to our fruitful discussions. This research was partially supported by the Strategic Japanese-  
151 German Cooperative Program from the Japan Science and Technology Agency and Deutsche  
152 Forschungsgemeinschaft, by a Grant-in-Aid for Young Scientists (B) (Grant No. 20710078),  
153 and also by a Grant-in-Aid for the Global COE "Center of Excellence for Atomically Con-  
154 trolled Fabrication Technology" from the Ministry of Education, Culture, Sports, Science  
155 and Technology, Japan. The numerical calculations were carried out using the computer  
156 facilities of the Institute for Solid State Physics at the University of Tokyo, the Center for  
157 Computational Sciences at University of Tsukuba, the Research Center for Computational  
158 Science at the National Institute of Natural Science, and the Information Synergy Center

159 at Tohoku University.

---

- 160 [1] H. Matsubara, T. Sasada, M. Takenaka, and S. Takagi, Appl. Phys. Lett. **93**, 032104 (2008).
- 161 [2] T. Hosoi, K. Kutsuki, G. Okamoto, M. Saito, T. Shimura, and H. Watanabe, Appl. Phys.  
162 Lett. **94**, 202112 (2009).
- 163 [3] T. Maeda, T. Yasuda, M. Nishizawa, N. Miyata, Y. Morita, and S. Takagi, Appl. Phys. Lett.  
164 **85**, 3181 (2004).
- 165 [4] V.V. Afanas'ev, Y.G. Fedorenko, and A. Stesmans, Appl. Phys. Lett. **87**, 032107 (2005).
- 166 [5] A. Delabie, F. Bellenger, M. Houssa, T. Conard, S. Van Elshocht, M. Caymax, M. Heyns, and  
167 M. Meuris, Appl. Phys. Lett. **91**, 082904 (2007).
- 168 [6] S. Takagi, T. Maeda, N. Taoka, M. Nishizawa, Y. Morita, K. Ikeda, Y. Yamashita, M.  
169 Nishikawa, H. Kumagai, R. Nakane, S. Sugahara, and N. Sugiyama, Microelect. Eng. **84**,  
170 2314 (2007).
- 171 [7] M. Houssa, G. Pourtois, M. Caymax, M. Meuris, M.M. Heyns, V.V. Afanas'ev, and A. Stes-  
172 mans, Appl. Phys. Lett. **93**, 161909 (2008).
- 173 [8] H. Kageshima and K. Shiraishi, Phys. Rev. Lett. **81**, 5936 (1998).
- 174 [9] S. Saito, T. Hosoi, H. Watanabe, and T. Ono, Appl. Phys. Lett. **95**, 011908 (2009).
- 175 [10] T. Watanabe, T. Onda, and I. Ohdomari, ECS Trans. **33**, 901 (2010).
- 176 [11] M. Yang, R.Q. Wu, Q. Chen, W.S. Deng, Y.P. Feng, J.W. Chai, J.S. Pan, and S.J. Wang,  
177 Appl. Phys. Lett. **94**, 142903 (2009).
- 178 [12] J.F. Binder, P. Broqvist, and A. Pasquarello, Microelect. Eng. **86**, 1760 (2009).
- 179 [13] P. Broqvist, J.F. Binder, and A. Pasquarello, Appl. Phys. Lett. **94**, 141911 (2009).
- 180 [14] M. Houssa, E.A. Chagarov and A.C. Kummel, MRS Bulletin **34**, 504 (2009).
- 181 [15] L. Tsetseris and S.T. Pantelides, Appl. Phys. Lett. **95**, 262107 (2009).
- 182 [16] J.R. Chelikowsky, N. Troullier, and Y. Saad, Phys. Rev. Lett. **72**, 1240 (1994); J.R. Che-  
183 likowsky, N. Troullier, K. Wu, and Y. Saad, Phys. Rev. B **50**, 11355 (1994).
- 184 [17] K. Hirose, T. Ono, Y. Fujimoto, and S. Tsukamoto, *First-Principles Calculations in Real-Space*  
185 *Formalism, Electronic Configurations and Transport Properties of Nanostructures* (Imperial  
186 College, London, 2005).
- 187 [18] T. Ono and K. Hirose, Phys. Rev. Lett. **82**, 5016 (1999); Phys. Rev. B **72**, 085115 (2005).

- 188 [19] We used the norm-conserving pseudopotentials NCPS97 constructed by K. Kobayashi; see K.  
189 Kobayashi, *Comput. Mater. Sci.* **14**, 72 (1999).
- 190 [20] N. Troullier and J.L. Martins, *Phys. Rev. B* **43**, 1993 (1991).
- 191 [21] L. Kleinman and D.M. Bylander, *Phys. Rev. Lett.* **48**, 1425 (1982).
- 192 [22] J.P. Perdew and A. Zunger, *Phys. Rev. B* **23**, 5048 (1981).
- 193 [23] T. Tamura, G-H. Lu, R. Yamamoto, and M. Kohyama, *Phys. Rev. B* **69**, 195204 (2004).
- 194 [24] T. Yamasaki, C. Kaneta, T. Uchiyama, T. Uda, and K. Terakura, *Phys. Rev. B* **63**, 115314  
195 (2001).
- 196 [25] The band gap of  $\sim 2.0$  eV ( $\sim 3.2$  eV) is estimated for the sixfold (fourfold) GeO<sub>2</sub> at the local  
197 density approximation level.

**FIGURES**

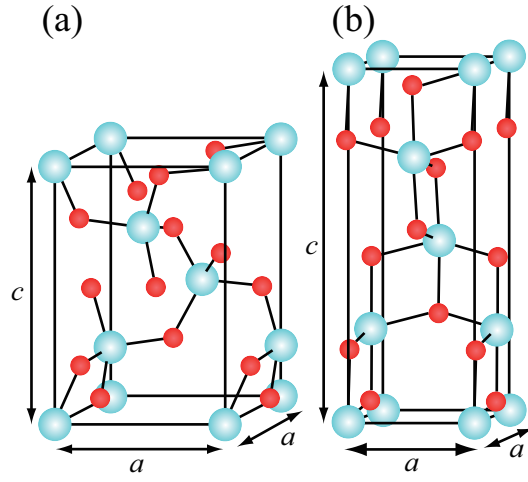


FIG. 1. (Color online) Unit cells of (a) fourfold and (b) sixfold  $c$ - $\text{GeO}_2$ . The solid cube represents the unit-cell volume, and the blue (light) and red (dark) circles are Ge and O atoms, respectively.

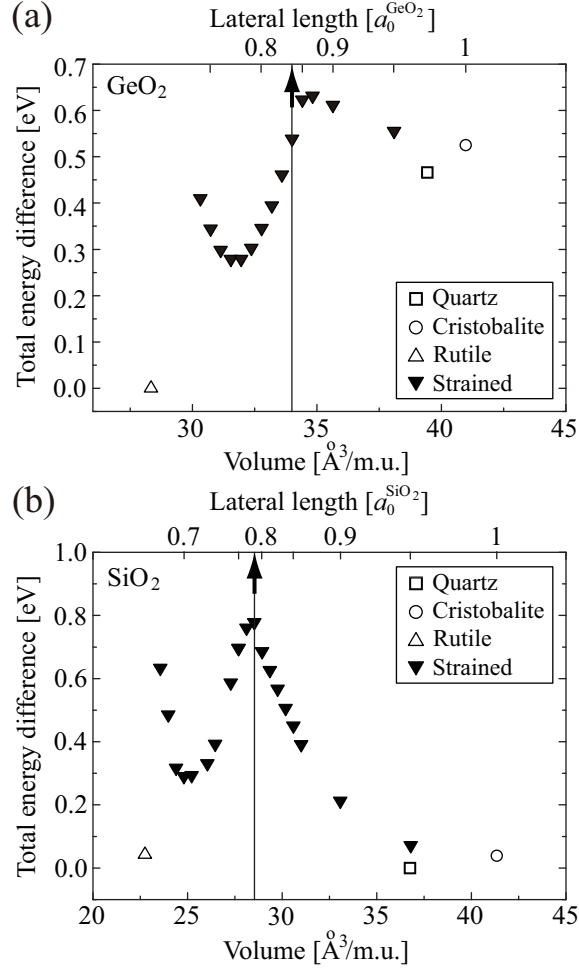


FIG. 2. Total energy per molecular unit (m.u.) as a function of volume for (a)  $c\text{-GeO}_2$  and (b)  $\text{SiO}_2$ . Energy minima of other phases [quartz ( $\square$ ), cristobalite ( $\circ$ ), and rutile ( $\triangle$ )] are also shown for comparison. The zero on the energy scale is rutile for  $\text{GeO}_2$  and quartz for  $\text{SiO}_2$ . The upper horizontal axes correspond to the lateral lengths of Ge and  $\text{Si}(001)\text{-}(1 \times 1)$  surfaces in  $a_0^{\text{GeO}_2}$  and  $a_0^{\text{SiO}_2}$ , where  $a_0^{\text{GeO}_2}$  and  $a_0^{\text{SiO}_2}$  represent the lengths of the  $a$ -axes of  $c\text{-GeO}_2$  and  $c\text{-SiO}_2$  at the equilibrium points, respectively.

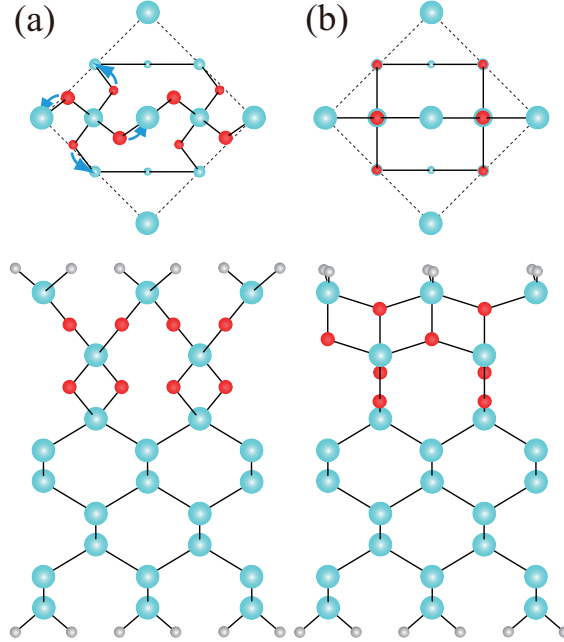


FIG. 3. (Color online) Top views and side views of (a) fourfold and (b) sixfold  $\text{GeO}_2/\text{Ge}(001)$  interfaces. The blue (light), red (dark), and grey (light small) circles are Ge, O, and H atoms, respectively. The dotted square in the top views represents a  $\text{Ge}(001)-(\sqrt{2} \times \sqrt{2})$  surface unit and the arrows indicate rotational directions to transform into sixfold structures.

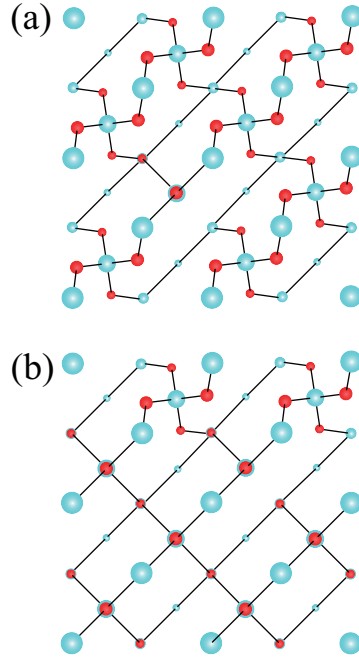


FIG. 4. (Color online) Top views of mixed fourfold and sixfold structures. (a) 12.5% and (b) 62.5% of Ge(001)-(1 × 1) surface units are composed of the sixfold structures. The blue (light) and red (dark) circles are Ge and O atoms, respectively.

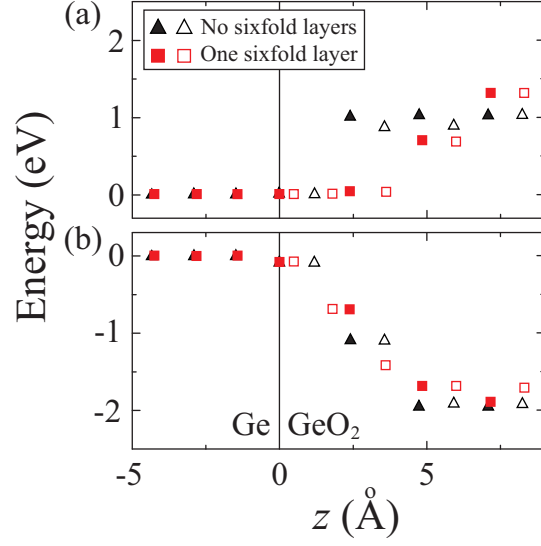


FIG. 5. (Color online) Variations of (a) CBM and (b) VBM along orthogonal direction to interface obtained on each atom. Triangles and squares are CBM and VBM of  $\text{GeO}_2/\text{Ge}$  interfaces with zero and one sixfold  $\text{GeO}_2$  layers, respectively. Filled (open) symbols represent CBM and VBM on Ge (O) atoms. Solid line indicates boundary between  $\text{GeO}_2$  and  $\text{Ge}(001)$  substrate.



200 **TABLES**

201

TABLE I. Lattice constants of  $c$ -GeO<sub>2</sub> and  $c$ -SiO<sub>2</sub> at their equilibrium points. The unit is Å

Structure	$a$	$c$
$c$ -GeO <sub>2</sub>	4.818	7.128
$c$ -SiO <sub>2</sub>	4.925	6.828

TABLE II. Energy difference between fully fourfold  $c$ -GeO<sub>2</sub> structure and various mixing ratios of fourfold and sixfold structures with respect to ratio of sixfold structure. All units are in eV.

Ratio of sixfold structure	0%	12.5%	62.5%	100%
	0	0.92	-0.49	-7.67